



A mixed interpolation-regression approximation operator on the triangle

Stefano De Marchi^a · Francesco Dell'Accio^{b,c} · Federico Nudo^a

Abstract

In several applications, ranging from computational geometry and finite element analysis to computer graphics, there is a need to approximate functions defined on triangular domains rather than rectangular ones. For this purpose, frequently used interpolation methods include barycentric interpolation, piecewise linear interpolation, and polynomial interpolation. However, the use of polynomial interpolation methods may suffer from the Runge phenomenon, affecting the accuracy of the approximation in the presence of equidistributed data. In these situations, the constrained mock-Chebyshev least squares approximation on rectangular domains was shown to be a successful approximation tool. In this paper, we extend it to triangular domains, by using both *Waldron and discrete Leja points*.

This paper is dedicated to Len Bos on the occasion of his retirement. Len, for us, is a master of mathematics and also a big friend. He introduced us to the fascinating world of "finding good interpolation nodes and effective interpolation strategies", mostly in the multivariate setting. The set of points we are using in this paper, Waldron and Leja, have been introduced to us by him and we hope that this note can be of some interest for him and all people working on approximation theory.

1 Introduction

In the field of computational sciences, a commonly encountered problem is the approximation of a function f , defined on a fixed interval $[a, b]$, through evaluations on a set of $n + 1$ points X_n , where n is a positive integer. Without loss of generality, we can assume we are working within the interval $[-1, 1]$. For this purpose, a widely adopted approach is polynomial interpolation, which entails determining a polynomial of degree at least n , $P_n[f] \in \mathbf{P}_n(\mathbb{R})$, that interpolates the function f at the points of X_n . A classical scenario of interest arises when X_n is the set of equispaced points in $[-1, 1]$

$$x_j = -1 + \frac{2j}{n}, \quad j = 0, \dots, n,$$

in correspondence of which the Runge phenomenon arises, demonstrating the inadequacy of such points to provide accurate approximations even in the case of local analytic functions f . To defeat the Runge phenomenon, various approaches have been proposed in recent years [2, 14, 15, 17, 32, 22]. A significant advancement is highlighted in the paper [14], which introduces the constrained mock-Chebyshev least squares approximation operator to enhance the precision of the method presented in [2]. Explicitly, the approximation proposed in [2], involves exclusively interpolating the function f on a subset of nodes near the Chebyshev–Lobatto nodes of a suitable order $m + 1 = \mathcal{O}(\sqrt{n})$. These nodes, denoted by $X'_m = \{x'_0, \dots, x'_m\}$, are referred as *mock-Chebyshev* nodes. However, this approach leaves several data points unused. Later on in [14], the authors introduced the constrained mock-Chebyshev least squares approximation, focusing on approximating the function f using a polynomial of degree $r > m$. The construction of this polynomial consists of interpolating f on the mock-Chebyshev nodes of order $m + 1$ and by using the remaining nodes to refine the accuracy through a simultaneous regression. In detail, for any function f defined on the discrete set X_n , the constrained mock-Chebyshev least squares polynomial $\hat{P}_{r,n}[f]$ is the solution of the problem

$$\|f - \hat{P}_{r,n}[f]\|_{X_n,2}^2 = \min_{P \in \mathbf{P}_r^*(\mathbb{R})} \|f - P\|_{X_n,2}^2, \quad (1)$$

where $\|\cdot\|_{X_n,2}$ is the discrete 2-norm on X_n and $\mathbf{P}_r^*(\mathbb{R})$ is the space formed by all polynomials of degree less than or equal to r interpolating f at the mock-Chebyshev nodes.

^aUniversity of Padova, Department of Mathematics "Tullio Levi-Civita", Italy

^bUniversity of Calabria, Department of Mathematics and Computer Science, Italy

^cIstituto per le Applicazioni del Calcolo "Mauro Picone", Naples Branch, C.N.R. National Research Council of Italy, Napoli, Italy

Setting

$$X''_{n-m} = X_n \setminus X'_m = \{x''_1, \dots, x''_{n-m}\},$$

we denote by $P_m[f] \in \mathbf{P}_m(\mathbb{R})$ the polynomial interpolating f at X'_m and by ω_m the nodal polynomial on X'_m , that is

$$\omega_m(x) = \prod_{i=0}^m (x - x'_i).$$

The constrained mock-Chebyshev least squares approximation can be then represented as

$$\hat{P}_{r,n}[f](x) = P_m[f](x) + Q_{n-m}(x)\omega_m(x),$$

where

$$\|\hat{f} - Q_{n-m}\|_{2,m}^2 = \min_{Q \in \mathbf{P}_{r-m-1}(\mathbb{R})} \|\hat{f} - Q\|_{2,m}^2, \quad (2)$$

and

$$\begin{aligned} \hat{f}(x) &= \frac{f(x) - P_m(x)}{\omega_m(x)}, \\ \|u\|_{2,m}^2 &= \sum_{k=1}^{n-m} \omega_m^2(x''_k) u^2(x''_k). \end{aligned} \quad (3)$$

Extending the constrained mock-Chebyshev least squares operator to the bivariate case necessitates the development of a new technique [22], which leverages the method of Lagrange multipliers to solve constrained least squares problems. By fixing a basis of the vector space $\mathbf{P}_r(\mathbb{R})$ say $B_r = \{u_0, \dots, u_r\}$, the approximation of f is expressed as

$$\hat{P}_{r,n}[f] = \sum_{i=0}^r a_i u_i$$

where $\mathbf{a} = [a_0, \dots, a_r]^T$ is the solution of *KKT-linear system* [22]. This method allows for constructing an accurate approximation of the function f on a domain of the type $R = [-1, 1]^d$, $d \geq 1$, by knowing only its evaluations on the regular Cartesian grid

$$\bigotimes_{k=1}^d X_{n_k} = \bigotimes_{k=1}^d \{x_0^{(k)}, \dots, x_{n_k}^{(k)}\}, \quad x_i^{(k)} = -1 + \frac{2}{n_k} i, \quad i = 0, \dots, n_k, \quad k = 1, \dots, d.$$

In recent years, the approximation method introduced in [14, 22], as well as other methods for defeating the Runge phenomenon, like [15], have found application in various contexts, as demonstrated by references [18, 23, 24, 25, 26, 27, 28]. However, in many applications, the function f is not defined on rectangular domains but preferably on triangles or more generally on simplices.

The interpolation process on triangles is widespread in computational geometry, finite element analysis, and computer graphics (see [12, 29] and references therein). The use of triangular meshes is a popular choice for representing complex geometries due to its efficiency in approximating irregular shapes. In practical applications, such as computed-aided geometric design or CAD, accurate interpolation on triangular domains is then crucial. It allows researchers and engineers to analyze and visualize data on surfaces, providing insights into physical phenomena or aiding in the design and optimization of structures. Overall, the interpolation of functions on triangular domains showcases the versatility of mathematical techniques in handling diverse geometric configurations and plays a pivotal role in advancing computational methods across various scientific and engineering disciplines.

Usually, the interpolating function is known only at a set of equidistributed points within a triangular domain. The stability of interpolation on such equidistributed points depends on several factors, including the chosen interpolation method, the regularity of the grid, and the smoothness of the function being approximated. When utilizing polynomial interpolation methods, the approximation can suffer from the Runge phenomenon. To address potential instability, exploring alternative interpolation methods could be worthwhile. Moreover, opting for higher-degree interpolation polynomials does not always guarantee better results; at times, lower-degree polynomials or alternative interpolation techniques might offer greater stability and accuracy [5]. In summary, while equidistributed points in a triangular domain can simplify interpolation, it is crucial to be mindful of potential stability issues. The selection of an interpolation method should strike a balance between accuracy and stability, considering the specific characteristics of the data and the requirements of the application.

Given the excellent results obtained using the constrained mock-Chebyshev least squares approximation in the case of rectangular domains, this paper aims to broaden this approximation to triangular domains in two different ways. We employ both *Waldron points* [8] and the well-known *discrete Leja points* [6] to guarantee precise and efficient interpolation.

The paper is organized as follows. In Section 2, we generalize the constrained mock-Chebyshev least squares approximation to triangular domains, introducing a new interpolation-regression method. In Section 3, we present some numerical results, demonstrating the accuracy of the proposed method.

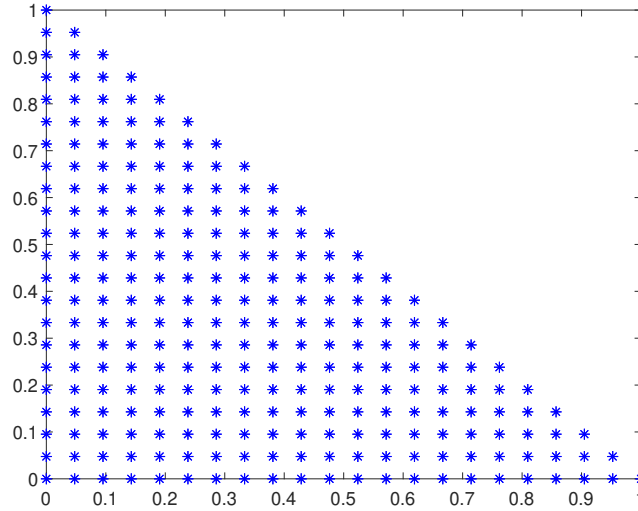


Figure 1: Plot of simplex points of degree $n = 21$ for the triangle T with vertices $v_1 = (0,0)$, $v_2 = (1,0)$, $v_3 = (0,1)$.

2 Interpolation-regression approximation on the triangle

2.1 Constrained mock-Waldron least squares approximation

Let $T \subset \mathbb{R}^2$ be a non-degenerate triangle with vertices v_1, v_2, v_3 . For any multi-index

$$\alpha = (\alpha_1, \alpha_2, \alpha_3) \in \mathbb{N}_0^3,$$

we denote by

$$|\alpha| = \sum_{i=1}^3 \alpha_i.$$

Moreover, we use

$$\kappa(l) = \binom{l+2}{2}, \quad (4)$$

to denote the dimension of the space of bivariate polynomials of degree $\leq l$.

Let f be an unknown function defined on T . We assume that we only know the evaluations of f at the simplex points of degree n , given by

$$X_n := \left\{ \mathbf{x}_\alpha = \sum_{i=1}^3 \frac{\alpha_i}{n} v_i : |\alpha| = n \right\}, \quad (5)$$

see Figure 1. We denote by $\mathbf{P}_n(\mathbb{R}^2)$ the space of polynomials of degree n in 2 variables. We observe that the cardinality of X_n is $N = \kappa(n)$. For this reason, we also write

$$X_n = \{\mathbf{x}_{\alpha_1}, \dots, \mathbf{x}_{\alpha_N}\}.$$

The goal of this subsection is to broaden the constrained mock-Chebyshev least squares approximation to triangular domains, presenting a novel interpolation-regression method. To achieve this, we need points capable of replacing the well-known Chebyshev–Lobatto nodes used in the domain $[-1, 1]$. The *Waldron points* [8] provide an example of points with these characteristics. Defining these points requires specifying an allowable weight function.

Definition 2.1. The function

$$\omega : [0, 1] \longrightarrow [0, 1], \quad (6)$$

is called an *allowable weight function* if it satisfies the following conditions:

- it is an increasing function;
- $\omega(0) = 0$ and $\omega(1) = 1$;
- for any non-negative θ_i , $i = 1, 2, 3$ and $\sum_{i=1}^3 \theta_i = 1$, the inequality $\sum_{i=1}^3 \omega(\theta_i) \leq 1$ is satisfied.

Remark 1. An example of allowable weight function is (cf. [8])

$$\omega(x) = \sin^2\left(\pi \frac{x}{2}\right). \quad (7)$$

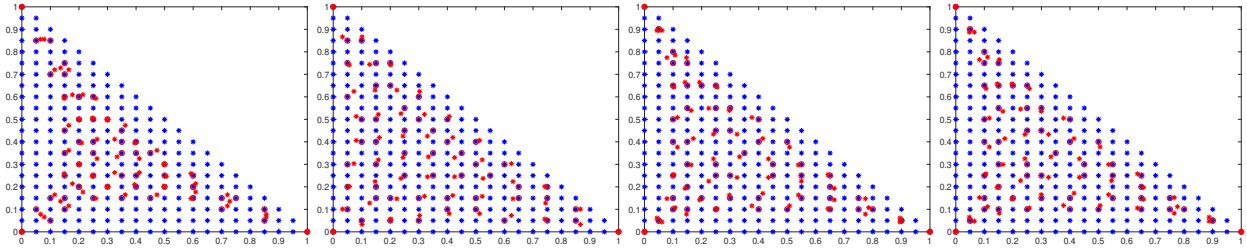


Figure 2: The discretization of the triangle with Waldron (*) and mock-Waldron (o) points for $n = 21$ for the weight functions ω_1 , with $k = 2$, ω_2 , ω_3 and ω_4 .

The following functions

$$\omega_1(x) = x^k \ (k \in \mathbb{N}), \quad \omega_2(x) = \frac{e^x - 1}{e - 1}, \quad \omega_3(x) = \left(\frac{\sin(x)}{\sin(1)} \right)^2, \quad \omega_4(x) = \frac{\log(x^2 + 1)}{\log(2)},$$

are also allowable weight functions. Indeed, they trivially satisfy the first two properties outlined in Definition 2.1. Moreover, since

$$\omega_i(x) \leq x, \quad x \in [0, 1], \quad i = 1, 2, 3, 4,$$

they fulfill the third property. We stress that Waldron points vary depending on the selected weight function. Throughout the paper, we use Waldron points corresponding to the weight function (7), as these points share the same density as the Chebyshev–Lobatto points on each side of the triangle while, by using the other weight functions, this property is lost (Fig. 2).

Definition 2.2. Let ω be an allowable weight function. The set of *Waldron points* of degree m for a triangle $T \subset \mathbb{R}^2$ with vertices $\mathbf{v}_1, \mathbf{v}_2, \mathbf{v}_3$ associated to ω is the set

$$W_m := \left\{ \mathbf{x}_\gamma^W = \sum_{j=1}^3 \omega_j \mathbf{v}_j : |\gamma| = m \right\}, \quad (8)$$

where

$$\omega_j := \omega\left(\frac{\gamma_j}{m}\right) + \frac{1}{3} \left(1 - \sum_{i=1}^3 \omega\left(\frac{\gamma_i}{m}\right) \right), \quad j = 1, 2, 3.$$

The cardinality of W_m is $M = \kappa(m)$, which corresponds to the dimension of the bivariate polynomials of total degree m . The points of W_m can be used to interpolate arbitrary data by polynomials of degree $\leq m$ in \mathbb{R}^2 [8].

The *mock-Waldron* approach for the triangle consists then of finding a suitable natural number $m < n$ such that we can uniquely identify M distinct points from X_n that are close to those of W_m . These points can be determined by a suitable nearest-neighbor algorithm and we denote the subset of *mock-Waldron* points by

$$W'_m = \{ \zeta_{\gamma_1}, \dots, \zeta_{\gamma_M} \} \subset X_n. \quad (9)$$

To determine the parameter m , we observe that the Waldron points associated with the weight function (7) exhibit the same density as the Chebyshev–Lobatto points on each side of the triangle, as illustrated in Figure 3. Therefore, following the approach proposed in [14, 22], we can set

$$m := \left\lfloor \pi \sqrt{\frac{n}{2}} \right\rfloor$$

as the greatest positive integer such that we can find, without repetitions, $\kappa(m)$ distinct nodes of X_n that are close to the Waldron points.

The fundamental idea behind this new interpolation-regression approximation is to approximate the function f with a bivariate polynomial of total degree r such that $m < r < n$, interpolating f at the mock-Waldron points of degree m , and leveraging the remaining nodes to improve the accuracy of the approximation through a simultaneous regression (see Figure 3). For these reasons, we refer to this new interpolation-regression approximation as the *constrained mock-Waldron least squares approximation*. To define this approximation, some settings are needed. We set

$$p := \left\lfloor \pi \sqrt{\frac{n}{12}} \right\rfloor, \quad r := m + p + 1, \quad R := \kappa(r).$$

We consider a basis of the polynomial space $\mathbf{P}_r(\mathbb{R}^2)$ given by

$$\mathcal{B}_r = \{ \mathbf{b}_{\beta_1}, \dots, \mathbf{b}_{\beta_R} \}, \quad (10)$$

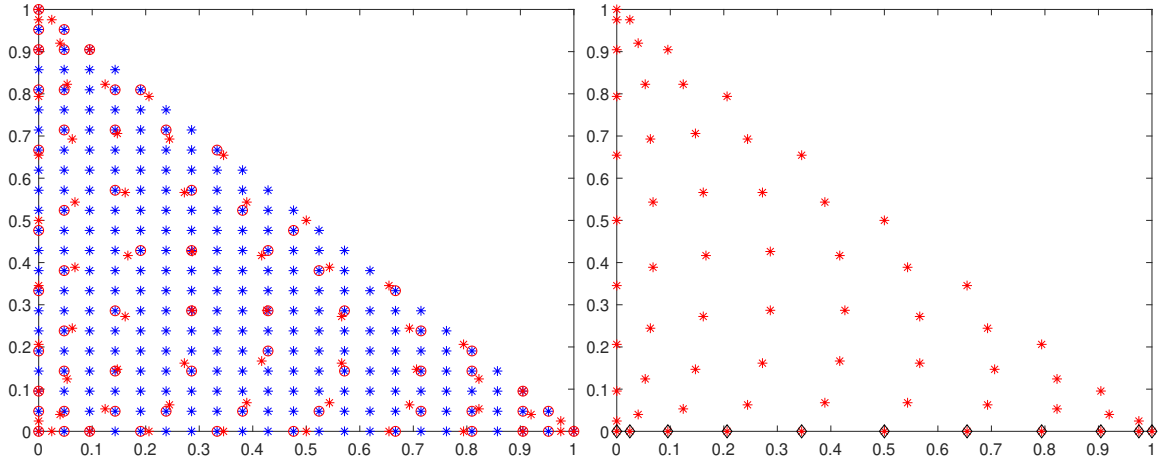


Figure 3: Left: The discretization of the triangle with Waldron (*) and mock-Waldron (o) points for $n = 21$. Right: Plot of Waldron points of degree $m = 10$ (*), and the scaled Chebyshev-Lobatto nodes on $[0, 1]$ (◇).

and, by assuming that

$$\text{span}\{\mathbf{b}_{\beta_1}, \dots, \mathbf{b}_{\beta_M}\} = \mathbf{P}_m(\mathbb{R}^2), \quad (11)$$

we set

$$\mathcal{B}_m = \{\mathbf{b}_{\beta_1}, \dots, \mathbf{b}_{\beta_M}\}.$$

For the sake of simplicity, we assume that the set X_n has been rearranged so that

$$\mathbf{x}_{a_i} = \zeta_{r_i}, \quad i = 1, \dots, M. \quad (12)$$

Let $A_{N,R} \in \mathbb{R}^{N \times R}$ be the interpolation matrix corresponding to \mathcal{B}_r and X_n , that is

$$A_{N,R} := \begin{bmatrix} \mathbf{b}_{\beta_1}(\mathbf{x}_{a_1}) & \mathbf{b}_{\beta_2}(\mathbf{x}_{a_1}) & \cdots & \mathbf{b}_{\beta_R}(\mathbf{x}_{a_1}) \\ \mathbf{b}_{\beta_1}(\mathbf{x}_{a_2}) & \mathbf{b}_{\beta_2}(\mathbf{x}_{a_2}) & \cdots & \mathbf{b}_{\beta_R}(\mathbf{x}_{a_2}) \\ \vdots & \vdots & \ddots & \vdots \\ \mathbf{b}_{\beta_1}(\mathbf{x}_{a_N}) & \mathbf{b}_{\beta_2}(\mathbf{x}_{a_N}) & \cdots & \mathbf{b}_{\beta_R}(\mathbf{x}_{a_N}) \end{bmatrix}. \quad (13)$$

We also denote by $A_{M,R} \in \mathbb{R}^{M \times R}$ the submatrix of $A_{N,R}$ formed by its first M rows, that is

$$A_{M,R} := \begin{bmatrix} \mathbf{b}_{\beta_1}(\mathbf{x}_{a_1}) & \mathbf{b}_{\beta_2}(\mathbf{x}_{a_1}) & \cdots & \mathbf{b}_{\beta_R}(\mathbf{x}_{a_1}) \\ \mathbf{b}_{\beta_1}(\mathbf{x}_{a_2}) & \mathbf{b}_{\beta_2}(\mathbf{x}_{a_2}) & \cdots & \mathbf{b}_{\beta_R}(\mathbf{x}_{a_2}) \\ \vdots & \vdots & \ddots & \vdots \\ \mathbf{b}_{\beta_1}(\mathbf{x}_{a_M}) & \mathbf{b}_{\beta_2}(\mathbf{x}_{a_M}) & \cdots & \mathbf{b}_{\beta_R}(\mathbf{x}_{a_M}) \end{bmatrix}. \quad (14)$$

Additionally, we set

$$\mathbf{a} := [f(\mathbf{x}_{a_1}), \dots, f(\mathbf{x}_{a_N})]^T, \quad \mathbf{d} := [f(\mathbf{x}_{a_1}), \dots, f(\mathbf{x}_{a_M})]^T$$

and

$$\mathbf{V} := A_{N,R}^T A_{N,R}, \quad \mathbf{v} := A_{N,R}^T \mathbf{a}. \quad (15)$$

Given assumptions (11) and (12), we can define the constrained mock-Waldron least squares approximation operator as follows

$$\begin{aligned} \hat{P}_{r,N}^W : C(T) &\longrightarrow \mathbf{P}_r(\mathbb{R}^2) \\ f &\longmapsto \hat{P}_{r,N}^W[f] := \sum_{i=1}^R c_i(f) \mathbf{b}_{\beta_i} \end{aligned} \quad (16)$$

where the vector of coefficients $\mathbf{c}(f) = [c_1(f), c_2(f), \dots, c_R(f)]^T$ is the solution of the linear system

$$\begin{bmatrix} 2\mathbf{V} & A_{M,R}^T \\ A_{M,R} & \mathbf{0} \end{bmatrix} \begin{bmatrix} \mathbf{c}(f) \\ \mathbf{z} \end{bmatrix} = \begin{bmatrix} 2\mathbf{v} \\ \mathbf{d} \end{bmatrix}. \quad (17)$$

Here, \mathbf{z} represents the vector of Lagrange multipliers.

The following theorem establishes the well-defined nature of the approximation operator (16).

Theorem 2.1. *The matrix*

$$\begin{bmatrix} 2V & A_{M,R}^T \\ A_{M,R} & 0 \end{bmatrix} \quad (18)$$

is nonsingular.

Proof. To establish this theorem, it suffices to demonstrate that the matrices $A_{N,R}$ and $A_{M,R}$, have maximum rank (cf. [4, Ch. 16]).

Let us consider the matrix $A_{N,R}$. By extending the basis $\mathcal{B}_r = \{\mathbf{b}_{\beta_1}, \dots, \mathbf{b}_{\beta_R}\}$ to the basis $\mathcal{B}_N = \{\mathbf{b}_{\beta_1}, \dots, \mathbf{b}_{\beta_R}, \mathbf{b}_{\beta_{R+1}}, \dots, \mathbf{b}_{\beta_N}\}$ of the vector space $\mathbf{P}_n(\mathbb{R}^2)$, we observe that $A_{N,R}$ is the submatrix $N \times R$ of the interpolation matrix

$$A_{N,N} := \begin{bmatrix} \mathbf{b}_{\beta_1}(\mathbf{x}_{a_1}) & \mathbf{b}_{\beta_2}(\mathbf{x}_{a_1}) & \cdots & \mathbf{b}_{\beta_N}(\mathbf{x}_{a_1}) \\ \mathbf{b}_{\beta_1}(\mathbf{x}_{a_2}) & \mathbf{b}_{\beta_2}(\mathbf{x}_{a_2}) & \cdots & \mathbf{b}_{\beta_N}(\mathbf{x}_{a_2}) \\ \vdots & \vdots & \ddots & \vdots \\ \mathbf{b}_{\beta_1}(\mathbf{x}_{a_N}) & \mathbf{b}_{\beta_2}(\mathbf{x}_{a_N}) & \cdots & \mathbf{b}_{\beta_N}(\mathbf{x}_{a_N}) \end{bmatrix}$$

made up of its first R columns. Since the simplex points (5) are unisolvent for the space $\mathbf{P}_n(\mathbb{R}^2)$, the matrix $A_{N,N}$ is nonsingular [10]. Therefore, its columns are linearly independent, and consequently, the columns of $A_{N,R}$ are linearly independent. Since $R < N$, the matrix $A_{N,R}$ has maximum rank.

Now, let us prove that the matrix $A_{M,R}$ has maximum rank. We observe that the submatrix of $A_{M,R}$ formed by its first M columns

$$A_{M,M} := \begin{bmatrix} \mathbf{b}_{\beta_1}(\mathbf{x}_{a_1}) & \mathbf{b}_{\beta_2}(\mathbf{x}_{a_1}) & \cdots & \mathbf{b}_{\beta_M}(\mathbf{x}_{a_1}) \\ \mathbf{b}_{\beta_1}(\mathbf{x}_{a_2}) & \mathbf{b}_{\beta_2}(\mathbf{x}_{a_2}) & \cdots & \mathbf{b}_{\beta_M}(\mathbf{x}_{a_2}) \\ \vdots & \vdots & \ddots & \vdots \\ \mathbf{b}_{\beta_1}(\mathbf{x}_{a_M}) & \mathbf{b}_{\beta_2}(\mathbf{x}_{a_M}) & \cdots & \mathbf{b}_{\beta_M}(\mathbf{x}_{a_M}) \end{bmatrix}$$

is nonsingular because the set of mock-Waldron points W'_m is unisolvent for the space $\mathbf{P}_m(\mathbb{R}^2)$ [34]. Therefore, its rows and the rows of the matrix $A_{M,R}$, are linearly independent. Being $R > M$, the matrix $A_{M,R}$ has maximum rank. \square

Remark 2. A direct implication of Theorem 2.1 is that, for any $f \in C(T)$, the coefficients of the polynomial $\hat{P}_{r,N}^W[f]$ are uniquely determined. Consequently, the approximation operator (16) is well-defined.

Remark 3. For any $f, g \in C(T)$ and $\alpha \in \mathbb{R}$, the operator $\hat{P}_{r,N}^W$ satisfies the following properties:

- $\hat{P}_{r,N}^W[f + g] = \hat{P}_{r,N}^W[f] + \hat{P}_{r,N}^W[g]$,
- $\hat{P}_{r,N}^W[\alpha f] = \alpha \hat{P}_{r,N}^W[f]$.

In other words, the operator $\hat{P}_{r,N}^W$ is a linear operator.

Remark 4. For any $p \in \mathbf{P}_r(\mathbb{R}^2)$, the operator $\hat{P}_{r,N}^W$ satisfies

$$\hat{P}_{r,N}^W[p] = p.$$

Moreover, we observe that

$$\hat{P}_{r,n}^W[f] = \hat{P}_{r,n}^W[P_n[f]], \quad (19)$$

where $P_n[f] \in \mathbf{P}_n(\mathbb{R}^2)$ is the polynomial interpolation of f on X_n . In simpler terms, the approximation $\hat{P}_{r,N}^W[f]$ relies solely on the evaluations of the function f on X_n .

Remark 5. Since $\hat{P}_{r,N}^W[f] \in \mathbf{P}_r(\mathbb{R}^2) \subset \mathbf{P}_n(\mathbb{R}^2)$, it can be expressed with respect to the Lagrange polynomial basis [10, Ch. 10]

$$\mathcal{L}_N = \{\ell_1(\mathbf{x}), \dots, \ell_N(\mathbf{x})\}$$

as follows

$$\hat{P}_{r,N}^W[f] = \sum_{i=1}^N L_{\mathbf{x}_{a_i}} \left(\hat{P}_{r,N}^W[f] \right) \ell_i(\mathbf{x}),$$

where $L_{\mathbf{x}_{a_i}}$ are the point evaluations functionals on X_n satisfying

$$L_{\mathbf{x}_{a_i}}(\ell_j) = \ell_j(\mathbf{x}_{a_i}) = \delta_{ij}.$$

The change of basis $\mathcal{L}_N \rightarrow \mathcal{B}_N$ allows us to write

$$\hat{P}_{r,N}^W[f] = \sum_{i=1}^N c_i \left(\hat{P}_{r,N}^W[f] \right) \mathbf{b}_{\beta_i} = \sum_{i=1}^R c_i(f) \mathbf{b}_{\beta_i},$$

since, by hypothesis, $\mathcal{B}_r = \{\mathbf{b}_{\beta_1}, \dots, \mathbf{b}_{\beta_R}\}$ spans $\mathbf{P}_r(\mathbb{R}^2)$. If \mathcal{B}_r is an orthonormal basis with respect to some inner product $\langle \cdot, \cdot \rangle$, we get

$$\langle \hat{P}_{r,N}^W[f], \mathbf{b}_{\beta_j} \rangle = \left\langle \sum_{i=1}^R c_i(f) \mathbf{b}_{\beta_i}, \mathbf{b}_{\beta_j} \right\rangle = \sum_{i=1}^R c_i(f) \langle \mathbf{b}_{\beta_i}, \mathbf{b}_{\beta_j} \rangle = c_j(f),$$

and then

$$\langle \hat{P}_{r,N}^W[f], \hat{P}_{r,N}^W[f] \rangle = \sum_{i=1}^R |c_i(f)|^2.$$

In the language of finite tight frames [35], we say that $c_i(f)$ are the canonical coordinates for $\hat{P}_{r,N}^W[f]$ with respect to the spanning sequence $\{\mathbf{b}_{\beta_1}, \dots, \mathbf{b}_{\beta_R}\}$ for the vector space $\mathbf{P}_r(\mathbb{R}^2)$.

Remark 6. The comparison between the constrained mock-Chebyshev least squares polynomial and the Lagrange polynomial interpolation on the nodes of X_n has been shown in the paper [22]. In the univariate case, it has been proved that the constrained mock-Chebyshev least squares polynomial improves the accuracy of the approximation of the mock-Chebyshev polynomial which, in its turn, defeats the Runge phenomenon due to the interpolation on the equispaced nodes. In the simplex case, the comparison between constrained mock-Chebyshev least squares polynomial and Lagrange interpolation polynomial on X_n shows an analogous behavior. In fact, the restrictions of these polynomials on the sides of the simplex are univariate polynomials of the same type.

2.2 Constrained Leja least squares approximation

The aim of this subsection is to modify the interpolation-regression method introduced in the previous section by using interpolation at discrete Leja points in the triangle [6], see Figure 4. These points share characteristics similar to Chebyshev–Lobatto points for the interval $[-1, 1]$ [13, 6, 7]. Hence, we refer to this new interpolation-regression method as the *constrained Leja least squares approximation*. The widely adopted set of discrete Leja points in polynomial interpolation has found application in various numerical contexts [31, 9, 11, 21, 20, 19]. These points are strategically chosen to enhance the stability and accuracy of the interpolation process, addressing potential numerical instability issues that could arise with certain node selections in specific interpolation scenarios [6]. The underlying concept is that Gaussian elimination with row pivoting performs a sort of greedy optimization of the Vandermonde determinant by iteratively selecting the new row in such a way that the modulus of the augmented determinant is maximized. Consequently, the discrete Leja points provide an unisolvent interpolation set with a low computational cost since a nonzero Vandermonde determinant is automatically sought. Moreover, since they are computed by greedy maximization, one can expect, as a qualitative guideline, that the condition number of the Vandermonde matrix does not increase rapidly and there is an improvement in the accuracy of the approximation interpolation polynomial [6]. The adoption of discrete Leja points is recognized for its significant contribution to establishing a more stable interpolation process, particularly beneficial for certain types of functions.

In the following discussion, we maintain the same notation as in the previous subsection. To define the constrained Leja least squares approximation, we assume that the basis \mathcal{B}_r of the polynomial space $\mathbf{P}_r(\mathbb{R}^2)$ satisfies the condition (11). Let

$$L_M = \{\xi_{\gamma_1}, \dots, \xi_{\gamma_M}\} \subset X_n$$

be a set of M discrete Leja points defined using the Greedy algorithm [6]. This process involves the use of the Vandermonde-type rectangular matrix $A_{N,M}$, associated with X_n and the basis \mathcal{B}_m , that is

$$A_{N,M} = \begin{bmatrix} \mathbf{b}_{\beta_1}(\mathbf{x}_{\alpha_1}) & \mathbf{b}_{\beta_2}(\mathbf{x}_{\alpha_1}) & \cdots & \mathbf{b}_{\beta_M}(\mathbf{x}_{\alpha_1}) \\ \mathbf{b}_{\beta_1}(\mathbf{x}_{\alpha_2}) & \mathbf{b}_{\beta_2}(\mathbf{x}_{\alpha_2}) & \cdots & \mathbf{b}_{\beta_M}(\mathbf{x}_{\alpha_2}) \\ \vdots & \vdots & \ddots & \vdots \\ \mathbf{b}_{\beta_1}(\mathbf{x}_{\alpha_N}) & \mathbf{b}_{\beta_2}(\mathbf{x}_{\alpha_N}) & \cdots & \mathbf{b}_{\beta_M}(\mathbf{x}_{\alpha_N}) \end{bmatrix}. \quad (20)$$

A Greedy maximization of nested square submatrix determinants, implemented through LU factorization with row pivoting of $A_{N,M}$, leads to the extraction of discrete Leja points from a *weakly admissible mesh* as outlined in [7, 6]. Since the set X_n defined in (5) is a weakly admissible mesh [16], the extraction of discrete Leja points from this set can be accomplished using the *Algorithm 1* [6].

In analogy to the previous subsection, for the sake of simplicity and brevity of notation, we assume that the set X_n has been rearranged, such that

$$\mathbf{x}_{\alpha_i} = \xi_{\gamma_i}, \quad i = 1, \dots, M. \quad (21)$$

Taking into account the assumptions (11) and (21), and in analogy to (16), we introduce the constrained Leja least squares approximation, denoted as $\hat{P}_{r,N}^L$. The fundamental idea behind the constrained Leja least squares approximation is to interpolate the function f at M discrete Leja points L_M and leverage the remaining nodes to improve the accuracy of the approximation through a simultaneous regression, see Figure 4.

Algorithm 1

Require: $X_n = [\mathbf{x}_{a_1}, \dots, \mathbf{x}_{a_N}]^T, \mathcal{B}_r = \{\mathbf{b}_{\beta_1}, \dots, \mathbf{b}_{\beta_R}\}$

Ensure: $L_M = [\xi_1, \dots, \xi_M]^T$

- 1: Compute N and M
- 2: $A_0 = A_{M,N}; k = 1 : N$
- 3: $[L_0, U_0, P_0] = \text{lu}(A_0); k = P_0 k;$
- 4: $L_m = [\xi_1, \dots, \xi_M] = X_n(i_1, \dots, i_M).$

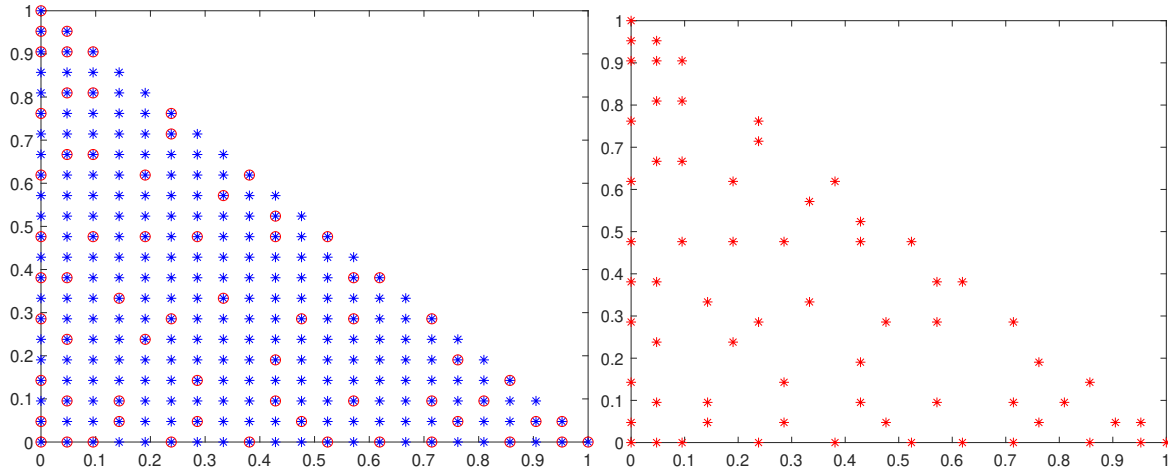


Figure 4: Left: Plot of simplex points of degree $n = 21$ (*) and $M = 66$ discrete Leja points with respect to the Koornwinder-Dubiner polynomial basis (o). Right: Plot of $M = 66$ discrete Leja points extracted from the uniform discretization of the unitary triangle T with vertices $\mathbf{v}_1 = (0, 0), \mathbf{v}_2 = (1, 0), \mathbf{v}_3 = (0, 1)$.

Remark 7. Taking into consideration the assumptions (11) and (21), we observe that the submatrix of $A_{M,R}$ formed by its first M columns

$$A_{M,M} := \begin{bmatrix} \mathbf{b}_{\beta_1}(\mathbf{x}_{a_1}) & \mathbf{b}_{\beta_2}(\mathbf{x}_{a_1}) & \dots & \mathbf{b}_{\beta_M}(\mathbf{x}_{a_1}) \\ \mathbf{b}_{\beta_1}(\mathbf{x}_{a_2}) & \mathbf{b}_{\beta_2}(\mathbf{x}_{a_2}) & \dots & \mathbf{b}_{\beta_M}(\mathbf{x}_{a_2}) \\ \vdots & \vdots & \ddots & \vdots \\ \mathbf{b}_{\beta_1}(\mathbf{x}_{a_M}) & \mathbf{b}_{\beta_2}(\mathbf{x}_{a_M}) & \dots & \mathbf{b}_{\beta_M}(\mathbf{x}_{a_M}) \end{bmatrix}$$

is nonsingular due to the unisolvency of the set of discrete Leja points L_M for the space $\mathbf{P}_m(\mathbb{R}^2)$. Consequently, its rows, and therefore the rows of the matrix $A_{M,R}$, are linearly independent. Since $R > M$, the matrix $A_{M,R}$ has maximum rank. Therefore, following the same approach of Theorem 2.1, the operator $\hat{P}_{r,n}^L$ is well-defined.

Remark 8. Since the constrained Leja least squares approximation is defined in the same way as the constrained mock-Waldron least squares approximation, it possesses the same properties.

3 Numerical experiments

In this section, we conduct numerical experiments to assess the accuracy of the proposed approximation method outlined in the previous section. We perform two types of numerical experiments. In the first type, we consider the following test functions

$$f_1(x, y) = \cos(10(x + y)), \quad f_2(x, y) = \frac{1}{x^2 + y^2 + 0.1}, \quad f_3(x, y) = \frac{e^{8(x-y)}}{x^3 + y^3 + 5}$$

$$f_4(x, y) = \sin(5\pi x) \cos(5\pi y), \quad f_5(x, y) = \frac{\sin(5\pi x)}{x^4 + y^4 + 25}, \quad f_6(x, y) = \log(x^6 + y^6 + 1).$$

For all experiments, we assume knowledge of the functions f_1 - f_6 on the grid of simplex points of degree $n = 40$ ($m = 14$). The approximations $\hat{P}_{r,N}^W[f]$, with respect to the weight function (7), and $\hat{P}_{r,N}^L[f]$ are expressed using the Koornwinder-Dubiner polynomial basis, constituting an orthogonal basis on the triangle T [33, 30]. The software to calculate the Koornwinder-Dubiner basis is available on the website <https://www.math.unipd.it/~alvise/sets.html>.

In Table 1 and Table 2, we compare the precision achieved by the interpolation operator at the mock-Waldron points W'_m , denoted as $P_m^W[f]$, with that obtained by the constrained mock-Waldron least squares approximation $\hat{P}_{r,N}^W[f]$ and with the interpolation operator on Waldron points of degree r , W_r . However, it should be noted that functional evaluations at these points

	Interpolation operator on W'_m	Interpolation-regression operator $\hat{P}_{r,N}^W$	Interpolation operator on W_r
f_1	4.7343e-08	3.6907e-12	3.4438e-11
f_2	1.2251e-05	2.0910e-07	3.5149e-07
f_3	1.3528e-05	2.1387e-09	1.1565e-08
f_4	3.4388e-02	6.3979e-04	1.2377e-03
f_5	4.0873e-06	4.4018e-10	2.2188e-09
f_6	2.0401e-08	1.7654e-10	2.0607e-09

Table 1: Comparison between the mean approximation error produced by interpolation operator at the mock-Waldron points W'_m , denoted by $P_m^W[f]$, with that produced by the interpolation-regression operator $\hat{P}_{r,N}^W[f]$ and with the interpolation operator at the Waldron points W_r .

are not available. Furthermore, since the density of the Waldron points on the x -axis is the same as that of the Chebyshev–Lobatto nodes, it is not possible to identify a subset of simplex points that emulate the behavior of the nodes of W_r in the mock-Chebyshev sense, as $r > m$ and m is the largest number for which this is possible. For more details, see [14].

The evaluations include the assessment of the maximum approximation error (e_{max}) and mean approximation error (e_{mean}), computed as follows:

$$e_{max} := \max_{i=1,\dots,N_e} r_i, \quad e_{mean} := \frac{1}{N_e} \sum_{i=1}^{N_e} r_i,$$

where r_i represents the absolute approximation error computed at the simplex points of degree $n_e = 131$, and $N_e = \kappa(n_e)$.

Similarly, in Table 3 and Table 4, we conduct the same experiments comparing the accuracy achieved by the interpolation operator at L_m , denoted as $P_m^L[f]$, with that obtained by the constrained Leja least squares approximation $\hat{P}_{r,N}^L[f]$. The evaluation metrics include the maximum approximation error (e_{max}) and mean approximation error (e_{mean}).

In all experiments, we observe that the approximation produced by $\hat{P}_{r,N}^W$ is of the same order of accuracy as that produced by $\hat{P}_{r,N}^L$. Additionally, in all experiments, we observe an enhancement in the approximation achieved by the operators $\hat{P}_{r,N}^W[f_i]$, $\hat{P}_{r,N}^L[f_i]$, $i = 1, \dots, 6$. In certain instances, this improvement is notably significant.

	Interpolation operator on W'_m	Interpolation-regression operator $\hat{P}_{r,N}^W$	Interpolation operator on W_r
f_1	2.6795e-07	1.1358e-10	1.2741e-09
f_2	1.1403e-04	7.4169e-06	7.7197e-06
f_3	3.7675e-04	4.1717e-07	3.3340e-07
f_4	4.1733e-01	6.2127e-02	2.5833e-02
f_5	1.8959e-05	8.4473e-09	8.7747e-08
f_6	7.5857e-08	3.6484e-09	3.8842e-08

Table 2: Comparison between the maximum approximation error produced by interpolation operator at the mock-Waldron points W'_m , denoted by $P_m^W[f]$, with that produced by the interpolation-regression operator $\hat{P}_{r,N}^W[f]$ and with the interpolation operator at the Waldron points W_r .

	Interpolation operator on L_m	Interpolation-regression operator $\hat{P}_{r,N}^L$
f_1	4.3280e-08	3.5227e-12
f_2	1.3689e-05	2.0706e-07
f_3	1.2287e-05	2.0370e-09
f_4	3.2576e-02	6.1144e-04
f_5	3.6089e-06	4.2373e-10
f_6	1.9039e-08	1.7599e-10

Table 3: Comparison between the mean approximation error produced by interpolation operator at the discrete Leja points L_m , denoted by $P_m^L[f]$, with that produced by the interpolation-regression operator $\hat{P}_{r,N}^L[f]$.

In the second type of experiment, we consider two different functions:

$$f_7(x, y) = \frac{1}{1 + 25(x^2 + y^2)}, \quad f_8(x, y) = \frac{1}{1 + 100\left(x - \frac{1}{3}\right)^2} \frac{1}{1 + 100\left(y - \frac{1}{3}\right)^2},$$

	Interpolation operator on L_m	Interpolation-regression operator $\hat{P}_{r,N}^L$
f_1	3.1048e-07	9.8591e-11
f_2	1.6461e-04	8.6597e-06
f_3	2.8134e-04	3.9013e-07
f_4	4.4848e-01	5.4833e-02
f_5	3.0969e-05	8.1826e-09
f_6	9.3728e-08	3.5562e-09

Table 4: Comparison between the maximum approximation error produced by interpolation operator at the discrete Leja points L_m , denoted by $P_m^L[f]$, with that produced by the interpolation-regression operator $\hat{P}_{r,N}^L[f]$.

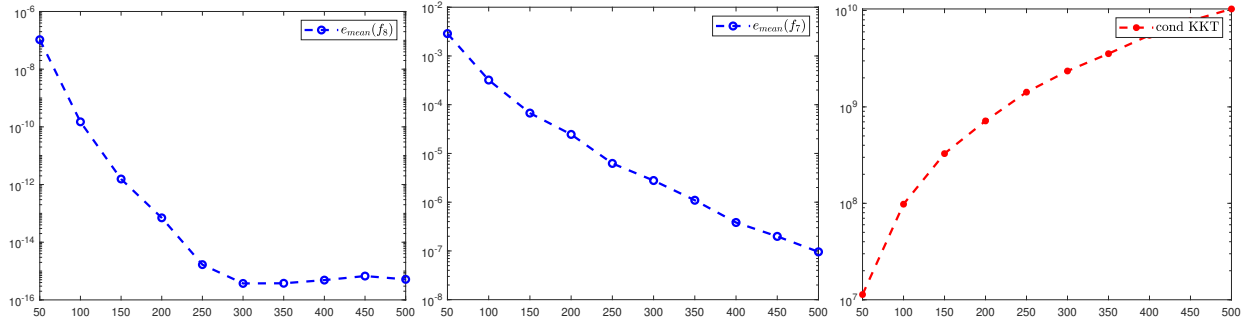


Figure 5: Plot of the mean approximation error for the functions f_7 (left) and f_8 (center), obtained using the constrained mock-Waldron least squares approximation with the Koornwinder-Dubiner polynomial basis, computed on a simplex of degree $n + 1 = 51 : 50 : 501$. Additionally, the condition number of the corresponding KKT matrix is shown (right).

the latter of which is defined in [3] to generalize the Runge function on a tetrahedron and was later used in [1] to find a Runge-like counterexample for 1-forms. We analyze the trend of the mean approximation errors produced by the constrained mock-Waldron least squares approximation relative to the Koornwinder-Dubiner polynomial basis. The results are shown in Figure 5.

We note that the results obtained are consistent with those found in the univariate case and in the bivariate rectangular domains. Specifically, we observe that the error trend decreases as n increases, and once the maximum precision is reached, it remains constant.

4 Conclusions and future work

In this paper, we extended the constrained mock-Chebyshev least squares approximation to triangular domains by using both Waldron and discrete Leja points. The results showcased here underscore the effectiveness of our method in addressing the unique challenges posed by triangular domains. Looking ahead, buoyed by the promising outcomes of this approach, our future aims are

- to find a suitable error estimation;
- to extend this approach to more general domains, such as polygonal or star-like in 2d or tetrahedral, pyramidal, conic sections, and cylindrical domains.

This endeavor builds upon our success on triangular domains and would seek to provide a versatile and robust polynomial approximation tool across a broader spectrum of applications.

Acknowledgments

This research has been achieved as part of RITA “Research Italian network on Approximation” and as part of the UMI group “Teoria dell’Approssimazione e Applicazioni”. The research was supported by GNCS-INdAM 2024 project “Metodi kernel e polinomiali per l’approssimazione e l’integrazione: teoria e software applicativo”. The authors are members of the INdAM-GNCS Research group. Project funded by the European Union-NextGenerationEU under the National Recovery and Resilience Plan (NRRP), Mission 4 Component 2 Investment 1.1 - Call PRIN 2022 No. 104 of February 2, 2022 of Italian Ministry of University and Research; Project 2022FHCNY3 (subject area: PE - Physical Sciences and Engineering) “Computational mEthods for Medical Imaging (CEMI)”.

References

- [1] A. Alonso Rodríguez, L. Bruni Bruno, and F. Rapetti. Whitney edge elements and the Runge phenomenon. *Journal of Computational and Applied Mathematics*, 427:115117, 2023.

- [2] J. P. Boyd, F. Xu. Divergence (Runge phenomenon) for least-squares polynomial approximation on an equispaced grid and Mock–Chebyshev subset interpolation. *Applied Mathematics and Computation*, 210:158–168, 2009.
- [3] M. G. Blyth, H. Luo, C. Pozrikidis. A comparison of interpolation grids over the triangle or the tetrahedron. *Journal of Engineering Mathematics*, 56:263–272, 2006.
- [4] S. Boyd, L. Vandenberghe. Introduction to applied linear algebra: vectors, matrices, and least squares. *Cambridge University Press*, 2018.
- [5] L. Bos, A. Sommariva, M. Vianello. Least-squares polynomial approximation on weakly admissible meshes: disk and triangle. *Journal of Computational and Applied Mathematics*, 235:660–668, 2010.
- [6] L. Bos, S. De Marchi, A. Sommariva, M. Vianello. Computing multivariate Fekete and Leja points by numerical linear algebra. *SIAM Journal on Numerical Analysis*, 48:1984–1999, 2010.
- [7] L. Bos, M. Caliari. Application of modified Leja sequences to polynomial interpolation. *Dolomites Research Notes on Approximation*, 8:66–74, 2015.
- [8] L. Bos, S. Ma’u, S. Waldron. On Waldron Interpolation on a Simplex in \mathbb{R}^d *arXiv preprint arXiv:2306.08392*, 2023.
- [9] D. Calvetti, L. Reichel. Adaptive Richardson iteration based on Leja points. *Journal of Computational and Applied Mathematics*, 71:267–286, 1996.
- [10] E. W. Cheney, W. A. Light. A course in approximation theory. *American Mathematical Society*, 2009.
- [11] D. I. Coroian, P. Dragnev. Constrained Leja points and the numerical solution of the constrained energy problem. *Journal of Computational and Applied Mathematics*, 131:427–444, 2001.
- [12] M. de Berg, O. Cheong, M. van Kreveld, M. Overmars. Computational Geometry: Algorithms and Applications. *Springer*, 2008.
- [13] S. De Marchi. On Leja sequences: some results and applications. *Applied Mathematics and Computation*, 152:621–647, 2004.
- [14] S. De Marchi, F. Dell’Accio, M. Mazza. On the constrained mock-Chebyshev least-squares. *Journal of Computational and Applied Mathematics*, 280:94–109, 2015.
- [15] S. De Marchi, F. Marchetti, E. Perracchione, D. Poggiali. Polynomial interpolation via mapped bases without resampling. *Journal of Computational and Applied Mathematics*, 364:112347, 2020.
- [16] L. Bos, S. De Marchi, A. Sommariva, M. Vianello. Weakly admissible meshes and discrete extremal sets. *Numerical Mathematics: Theory, methods and applications*, 4:1–12, 2011.
- [17] S. De Marchi, F. Marchetti, E. Perracchione, D. Poggiali. Multivariate approximation at fake nodes. *Applied Mathematics and Computation*, 391:125628, 2021.
- [18] S. De Marchi, G. Elefante, E. Perracchione, D. Poggiali. Quadrature at fake nodes. *Dolomites Research Notes on Approximation*, 14:39–45, 2021.
- [19] R. Cavoretto, A. De Rossi, F. Dell’Accio, F. Di Tommaso, N. Siar, A. Sommariva, M. Vianello. Numerical cubature on scattered data by adaptive interpolation. *Journal of Computational and Applied Mathematics*, 444:115793, 2024.
- [20] F. Dell’Accio, F. Di Tommaso, N. Siar, M. Vianello. Numerical differentiation on scattered data through multivariate polynomial interpolation. *BIT Numerical Mathematics*, 62:773–801, 2022.
- [21] F. Dell’Accio, F. Di Tommaso, O. Nouisser, N. Siar. Solving Poisson equation with Dirichlet conditions through multinode Shepard operators. *Computers & Mathematics with Applications*, 98:254–260, 2021.
- [22] F. Dell’Accio, F. Di Tommaso, F. Nudo. Generalizations of the constrained mock-Chebyshev least squares in two variables: Tensor product vs total degree polynomial interpolation. *Applied Mathematics Letters*, 125:107732, 2022.
- [23] F. Dell’Accio, F. Di Tommaso, F. Nudo. Constrained mock-Chebyshev least squares quadrature. *Applied Mathematics Letters*, 134:108328, 2022.
- [24] F. Dell’Accio, F. Di Tommaso, E. Francomano, F. Nudo. An adaptive algorithm for determining the optimal degree of regression in constrained mock-Chebyshev least squares quadrature. *Dolomites Research Notes on Approximation*, 15:35–44, 2022.
- [25] F. Dell’Accio, D. Mezzanotte, F. Nudo, D. Occorsio. Product integration rules by the constrained mock-Chebyshev least squares operator. *BIT Numerical Mathematics*, 63:24, 2023.
- [26] F. Dell’Accio, F. Nudo. Polynomial approximation of derivatives through a regression-interpolation method. *Applied Mathematics Letters*, 152:109010, 2024.
- [27] F. Dell’Accio, D. Mezzanotte, F. Nudo, D. Occorsio. Numerical approximation of Fredholm integral equation by the constrained mock-Chebyshev least squares operator. *Journal of Computational and Applied Mathematics*, 447:115886, 2024.
- [28] F. Dell’Accio, F. Marcellán, F. Nudo. An extension of a mixed interpolation-regression method using zeros of orthogonal polynomials. *Journal of Computational and Applied Mathematics*, 450:116010, 2024.
- [29] J. Hoschek, D. Lasser. Fundamentals of Computer Aided Geometric Design. *A K Peters/CRC Press*, 1996.
- [30] F. Rapetti, A. Sommariva, M. Vianello. On the generation of symmetric Lebesgue-like points in the triangle. *Journal of Computational and Applied Mathematics*, 236:4925–4932, 2012.
- [31] L. Reichel. The application of Leja points to Richardson iteration and polynomial preconditioning. *Linear Algebra and its Applications*, 154:389–414, 1991.

-
- [32] D. Occorsio, G. Ramella, W. Themistoclakis. Lagrange–Chebyshev Interpolation for image resizing. *Mathematics and Computers in Simulation*, 197:105–126, 2022.
- [33] R. Pasquetti, F. Rapetti. Spectral element methods on triangles and quadrilaterals: comparisons and applications. *Journal of Computational Physics*, 198:349–362, 2004.
- [34] M. Vianello. Dubiner distance and stability of Lebesgue constants. *Journal of Inequalities and Special Functions*, 10:49–60, 2019.
- [35] S. Waldron. An introduction to finite tight frames. *Birkhäuser*, 2018.